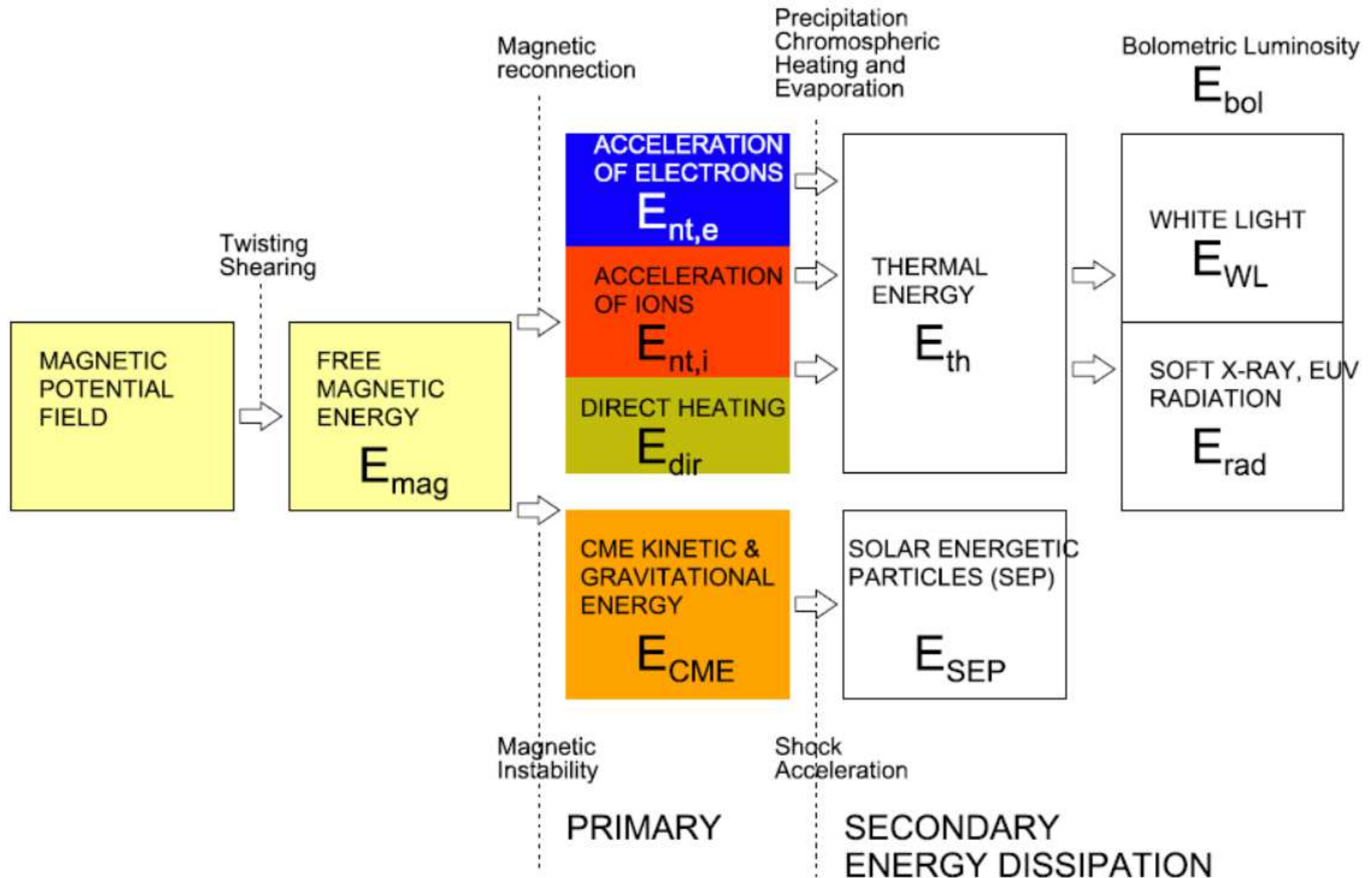
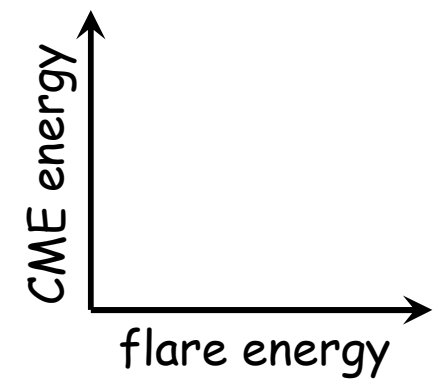
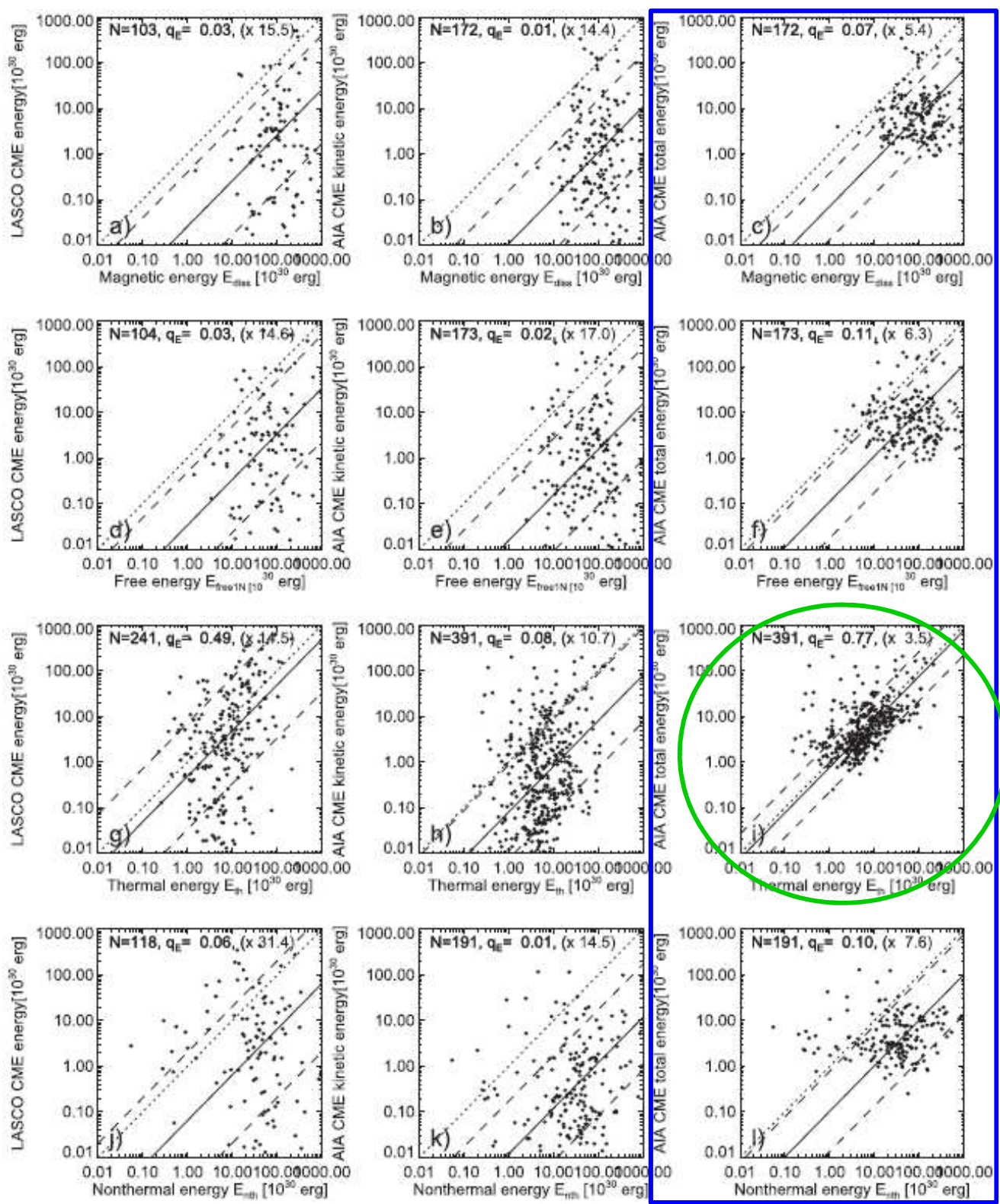


Global Energetics

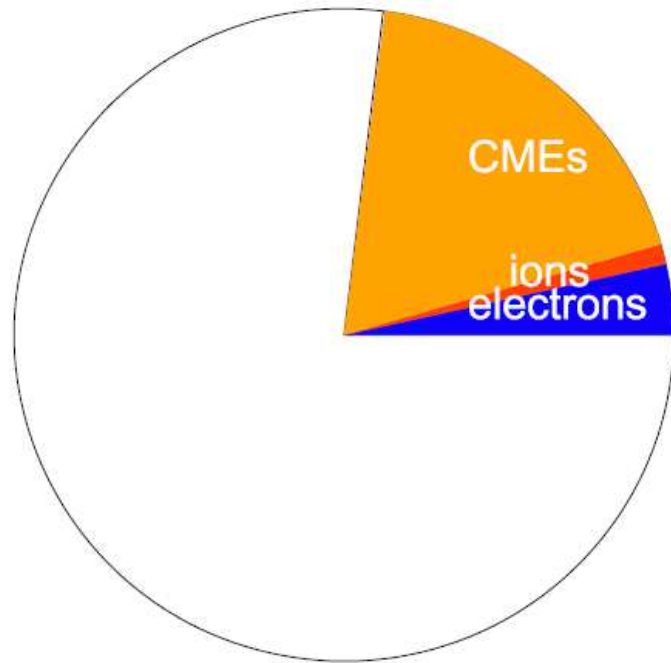




It is imperial to include both the kinetic and gravitational energy in comparisons with other flare-generated energies.

The energy that goes into a CME is most closely related to the heating of the flare plasma.

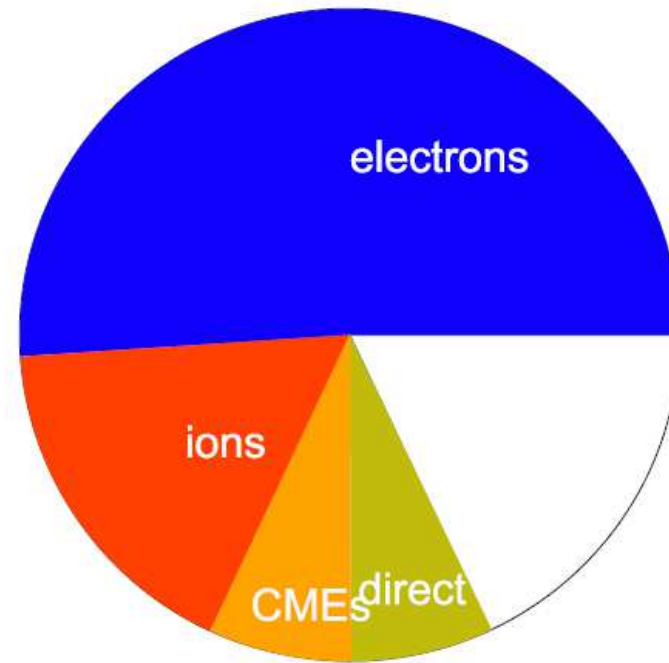
Emslie et al. (2012)



Elec/magnetic energy = 0.04+0.17
Ions/magnetic energy = 0.01+0.48
CME/magnetic energy = 0.19+0.20

ENERGY CLOSURE :
Sum/magnetic energy = 0.25+0.24

This study (2016)



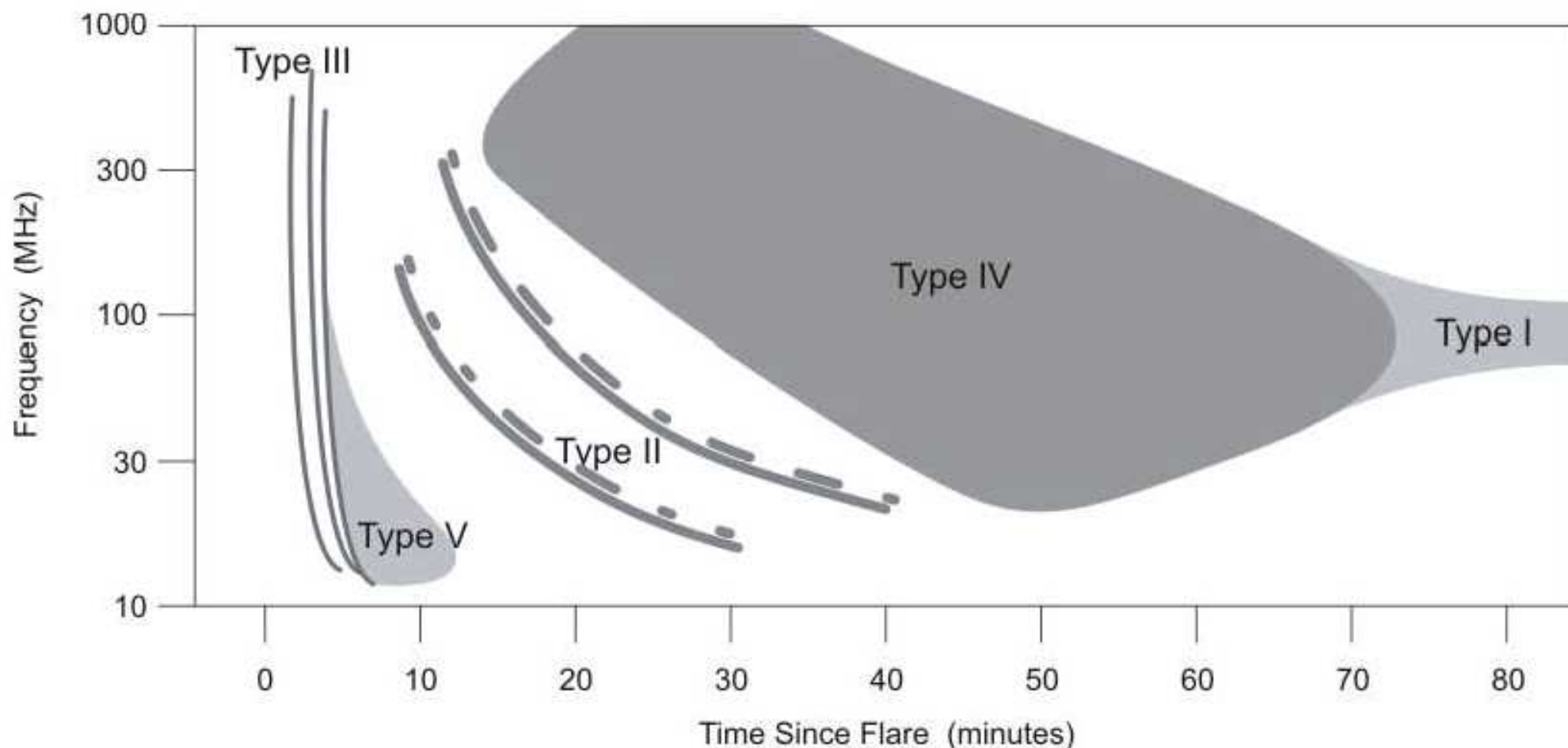
Elec/magnetic energy = 0.51+0.17
Ions/magnetic energy = 0.17+0.17
CME/magnetic energy = 0.07+0.14
direct/magnetic energy = 0.07+0.17

ENERGY CLOSURE :
Sum/magnetic energy = 0.87+0.18

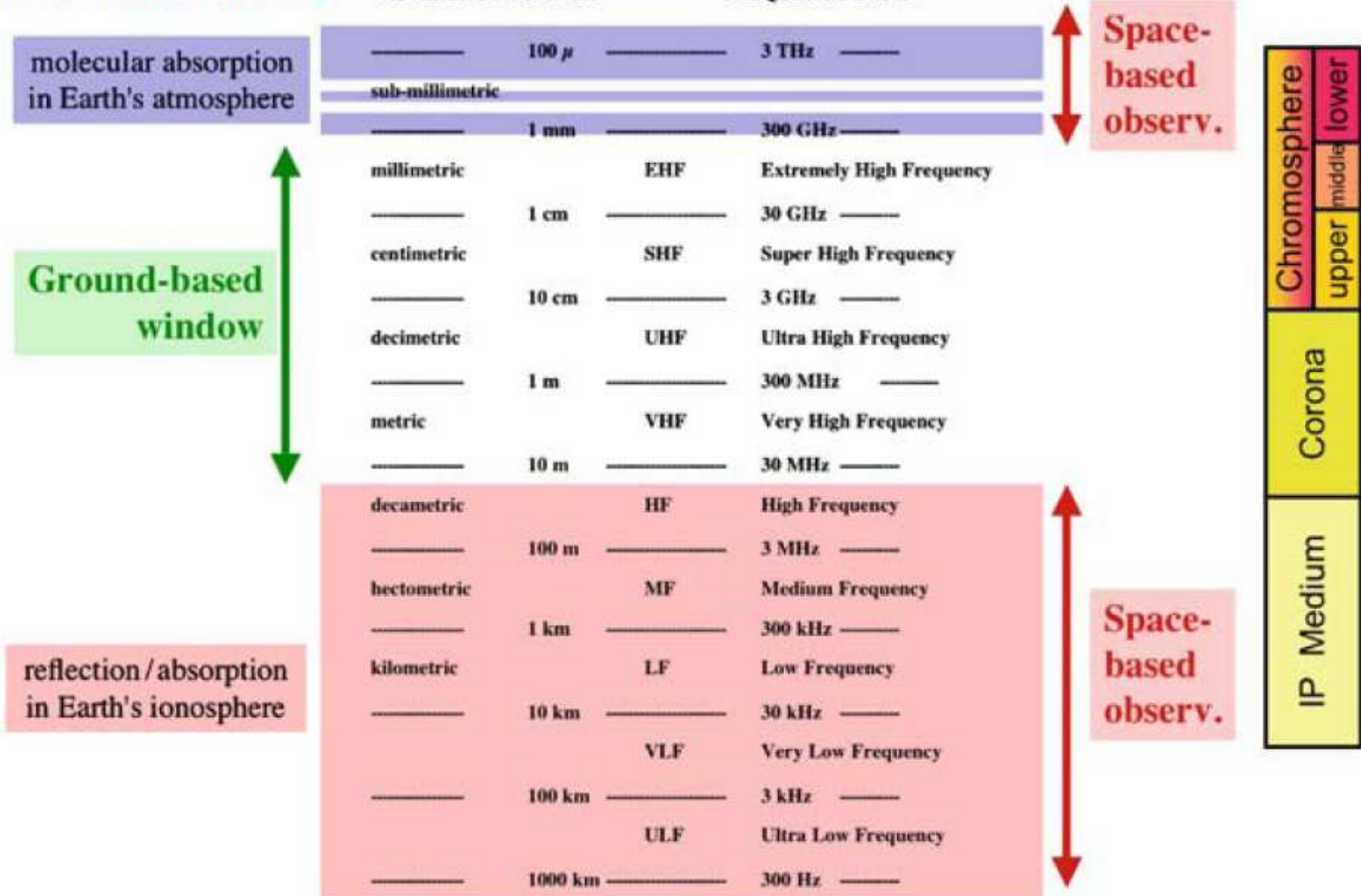
Solar Radio Bursts

Schematic Radiospectrogram

This diagram illustrates all of the major burst types in a typical configuration following a large flare. It should be noted that it is **not** common for **all** of these features to be observed after a flare.



The radio band



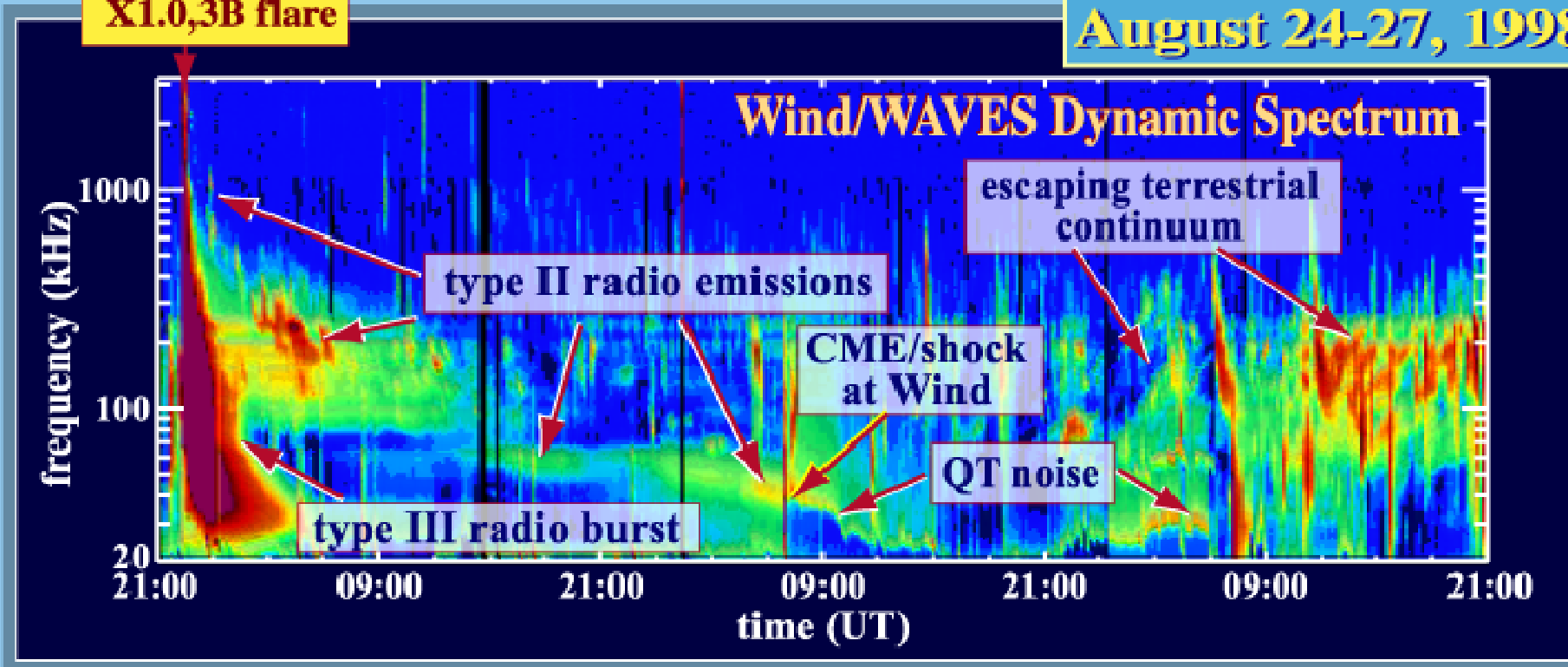
→ The shorter wavelengths are absorbed in the Earth's atmosphere and the longer wavelengths are blocked by the terrestrial ionosphere.

Fig. 6.1 & Fig. 6.2 in Yohsuke Kamide & Abraham C.-L. Chian (2007)

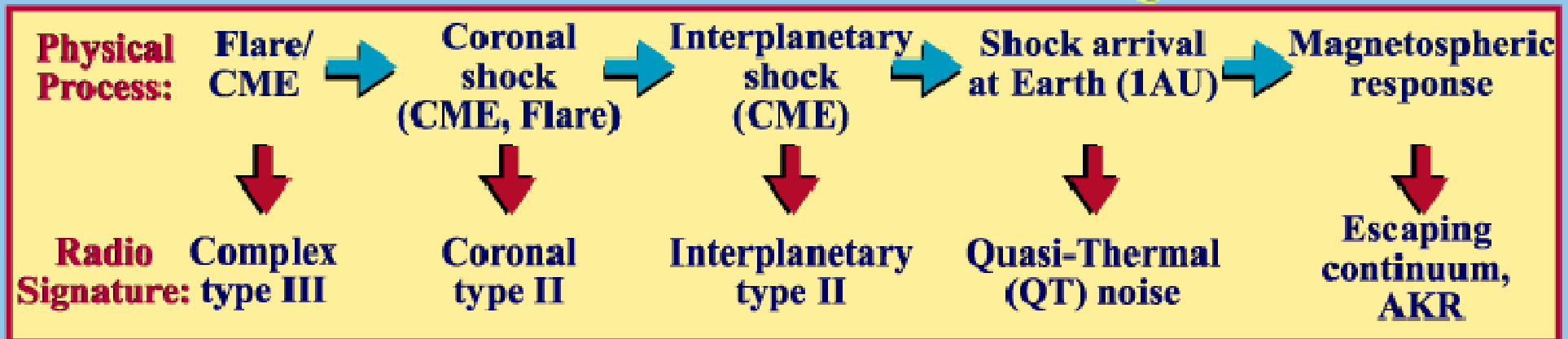
Radio Signatures of a Solar-Terrestrial Event

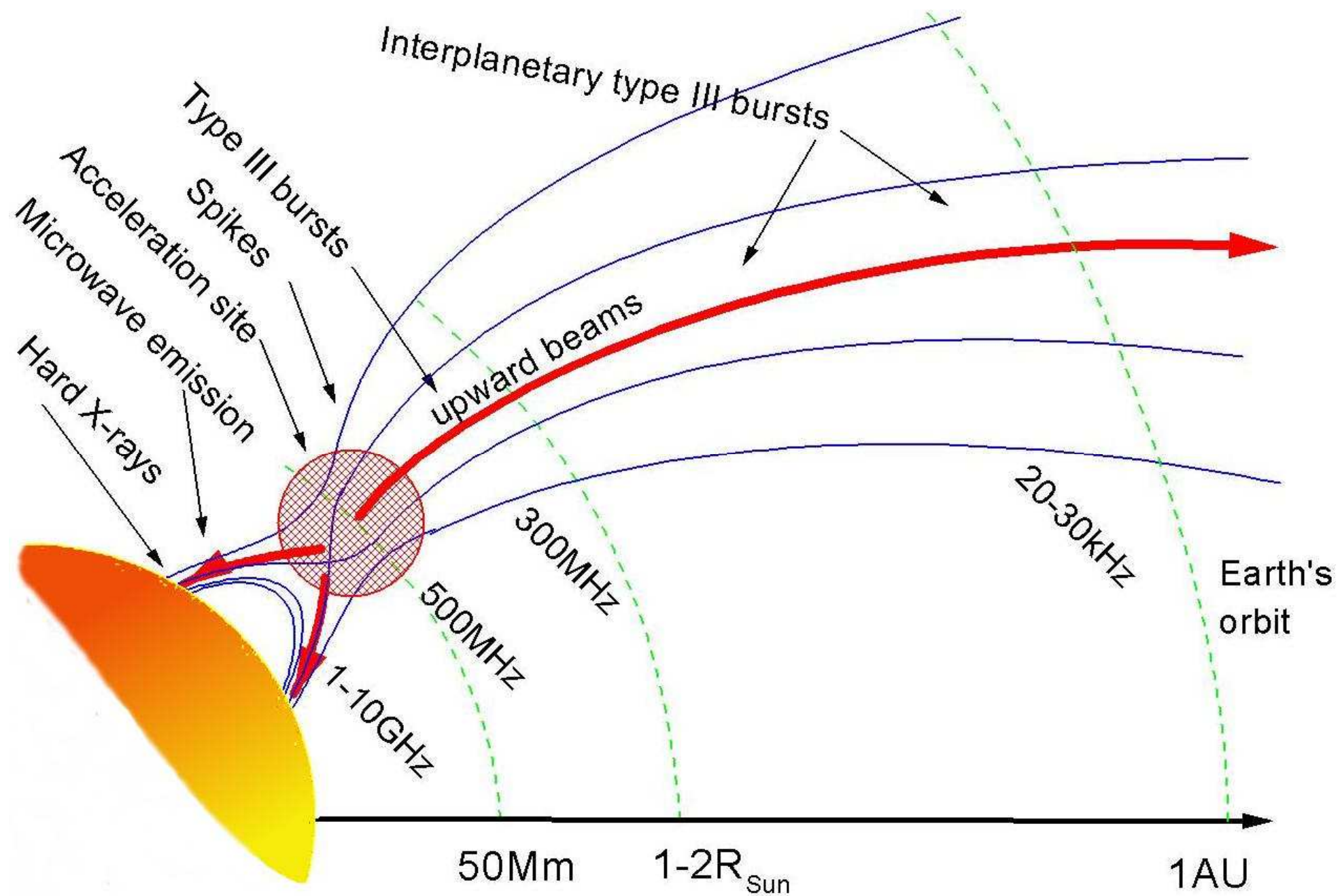
X1.0,3B flare

August 24-27, 1998



Solar - Terrestrial Radio Paradigm





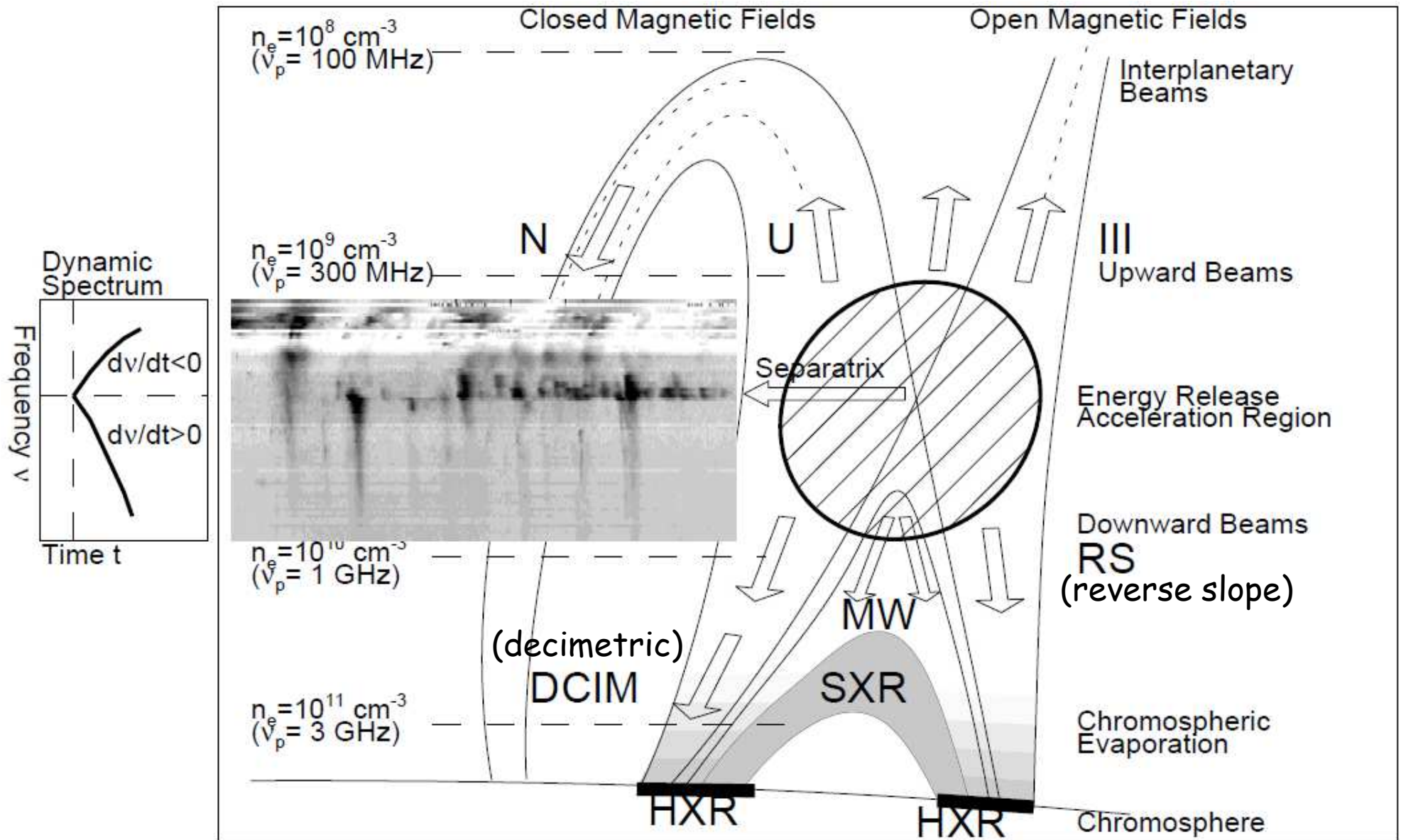
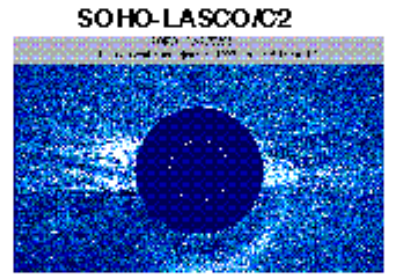
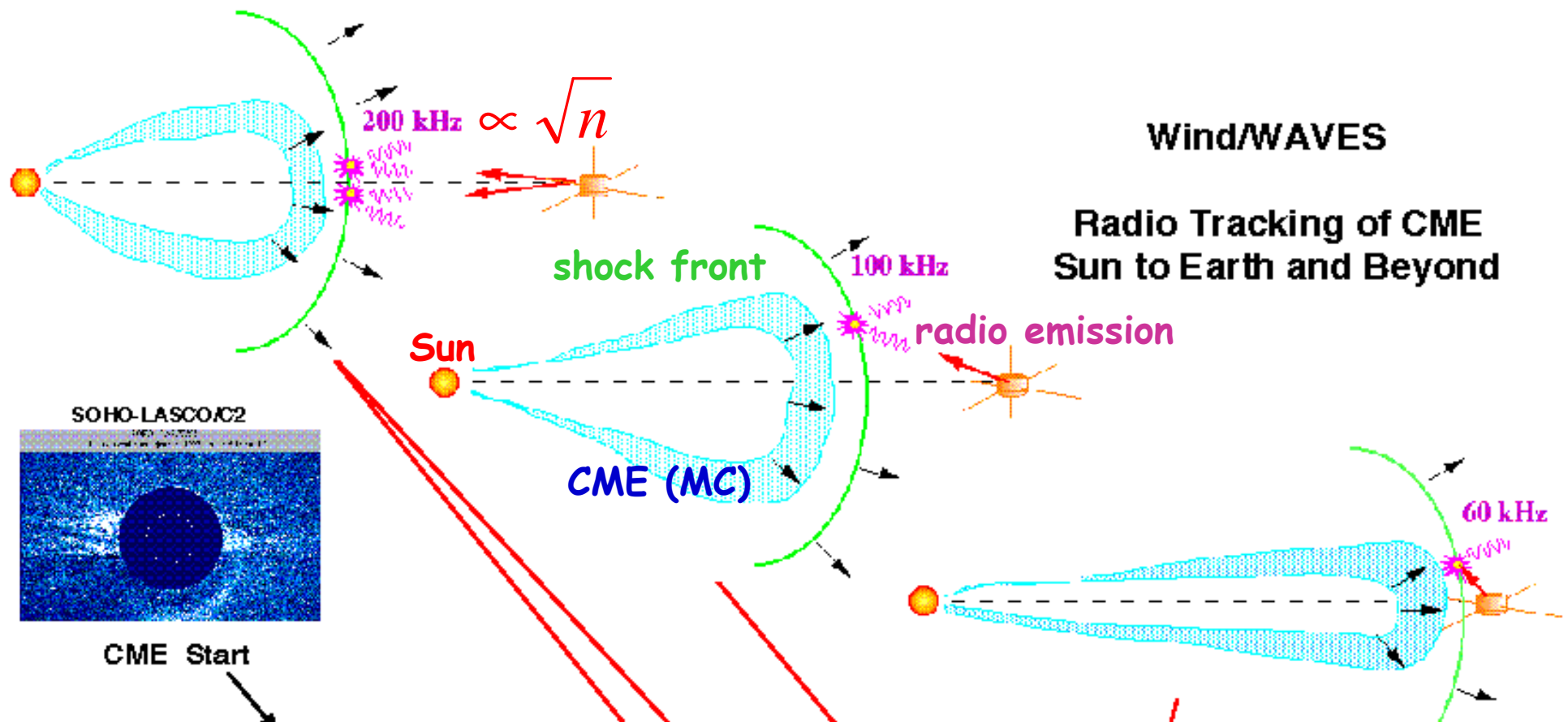


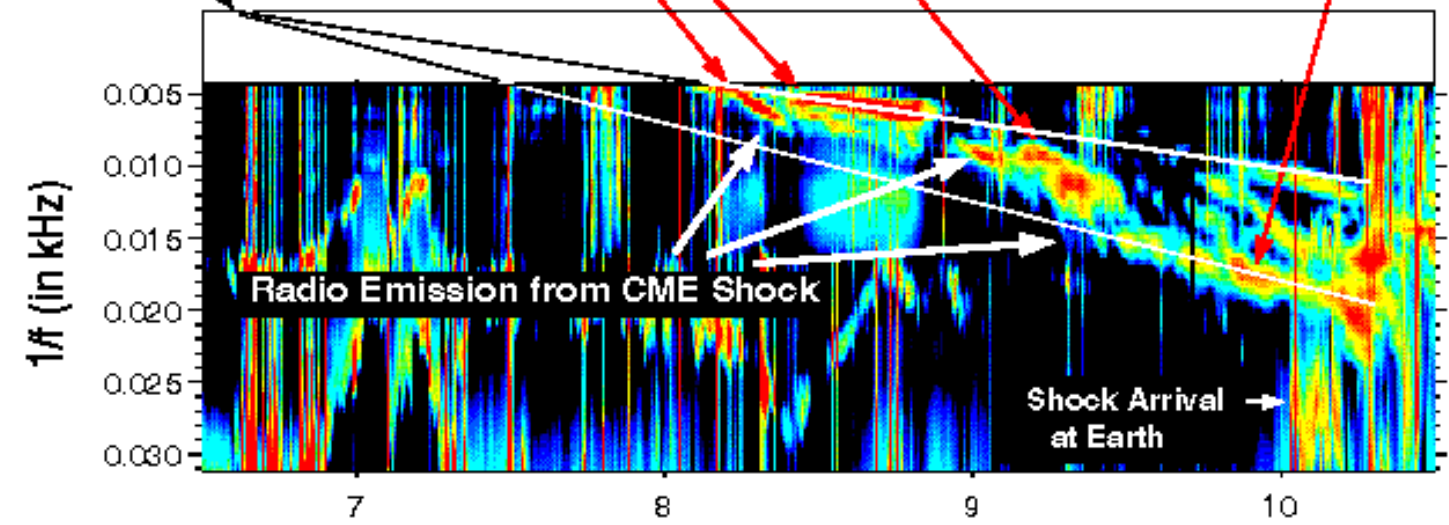
Fig. 15.15 in Markus J. Aschwanden (2005)

Wind/WAVES

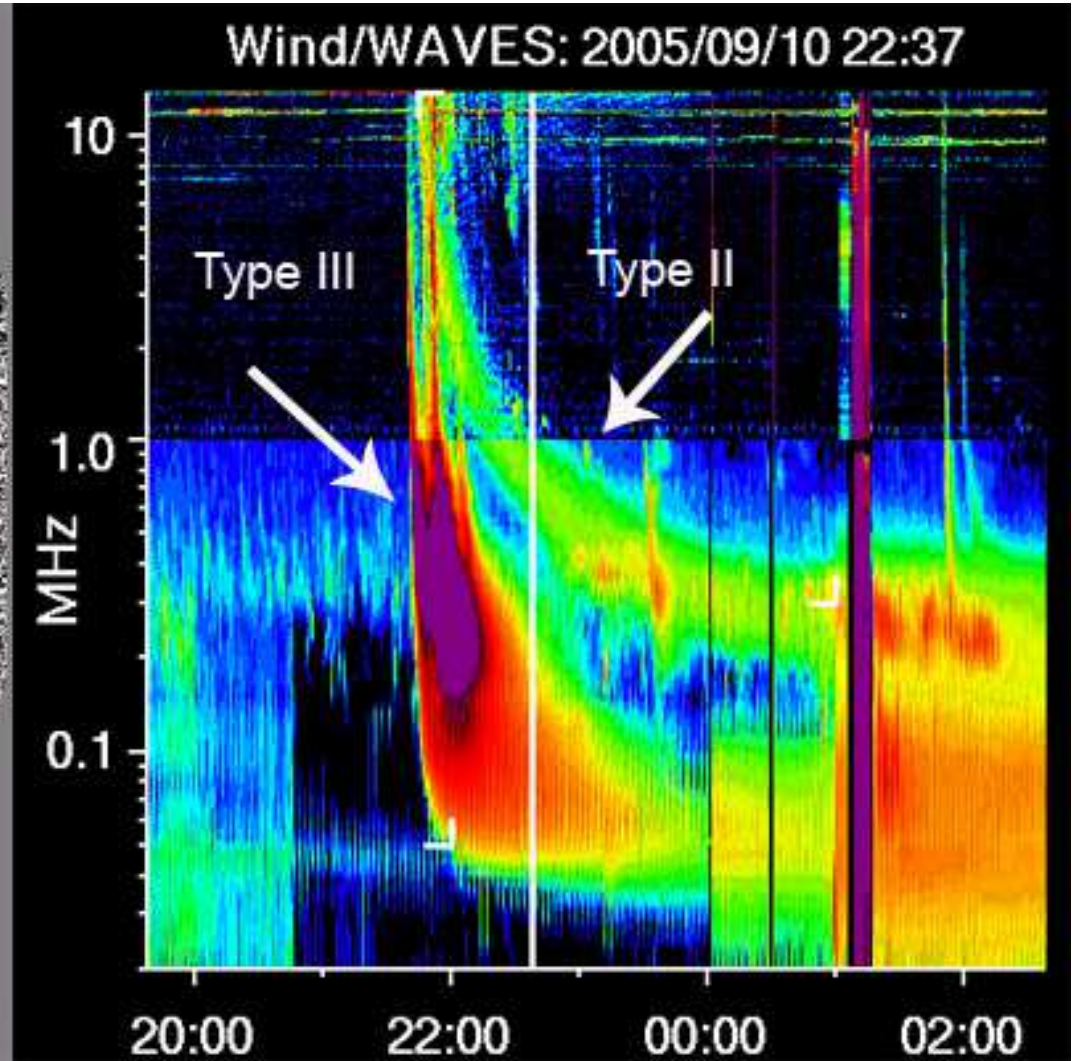
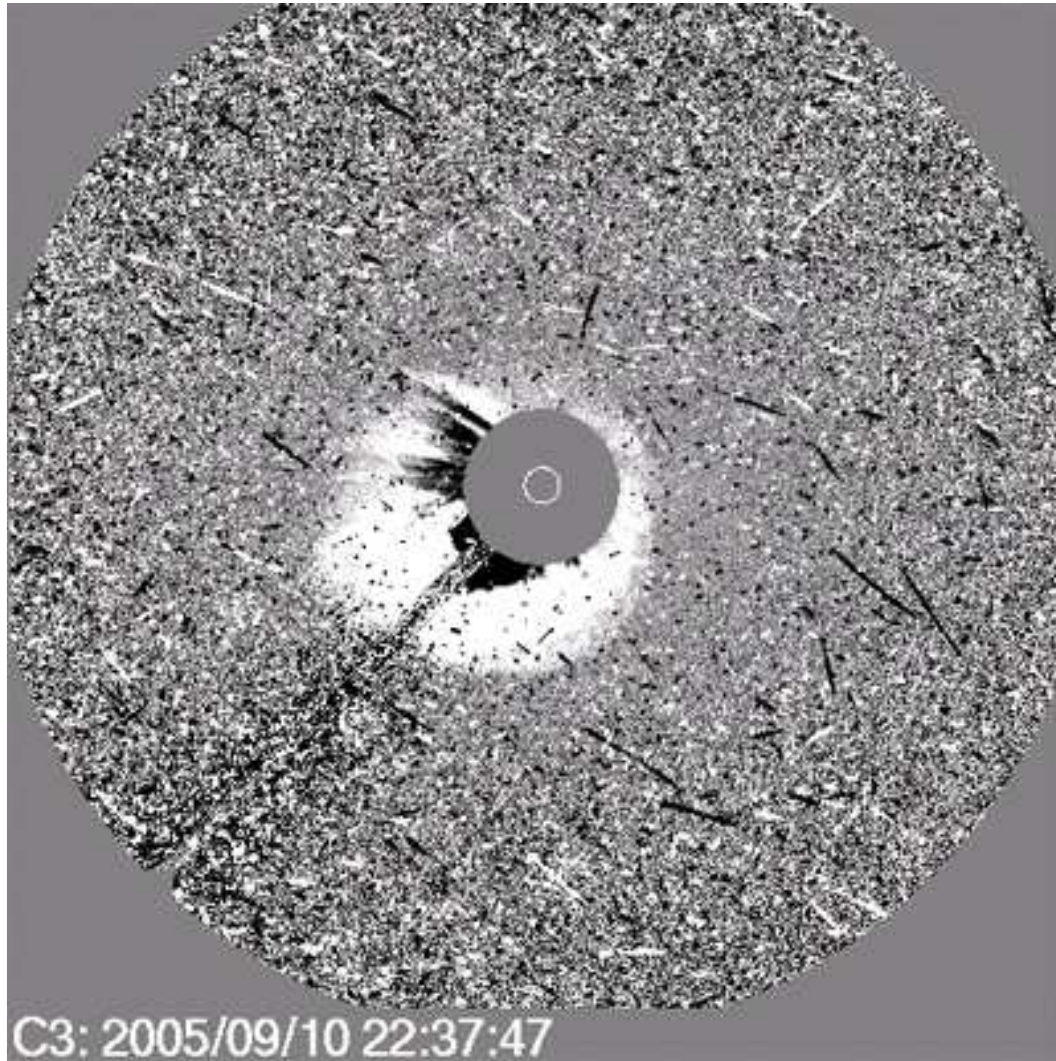
Radio Tracking of CME Sun to Earth and Beyond

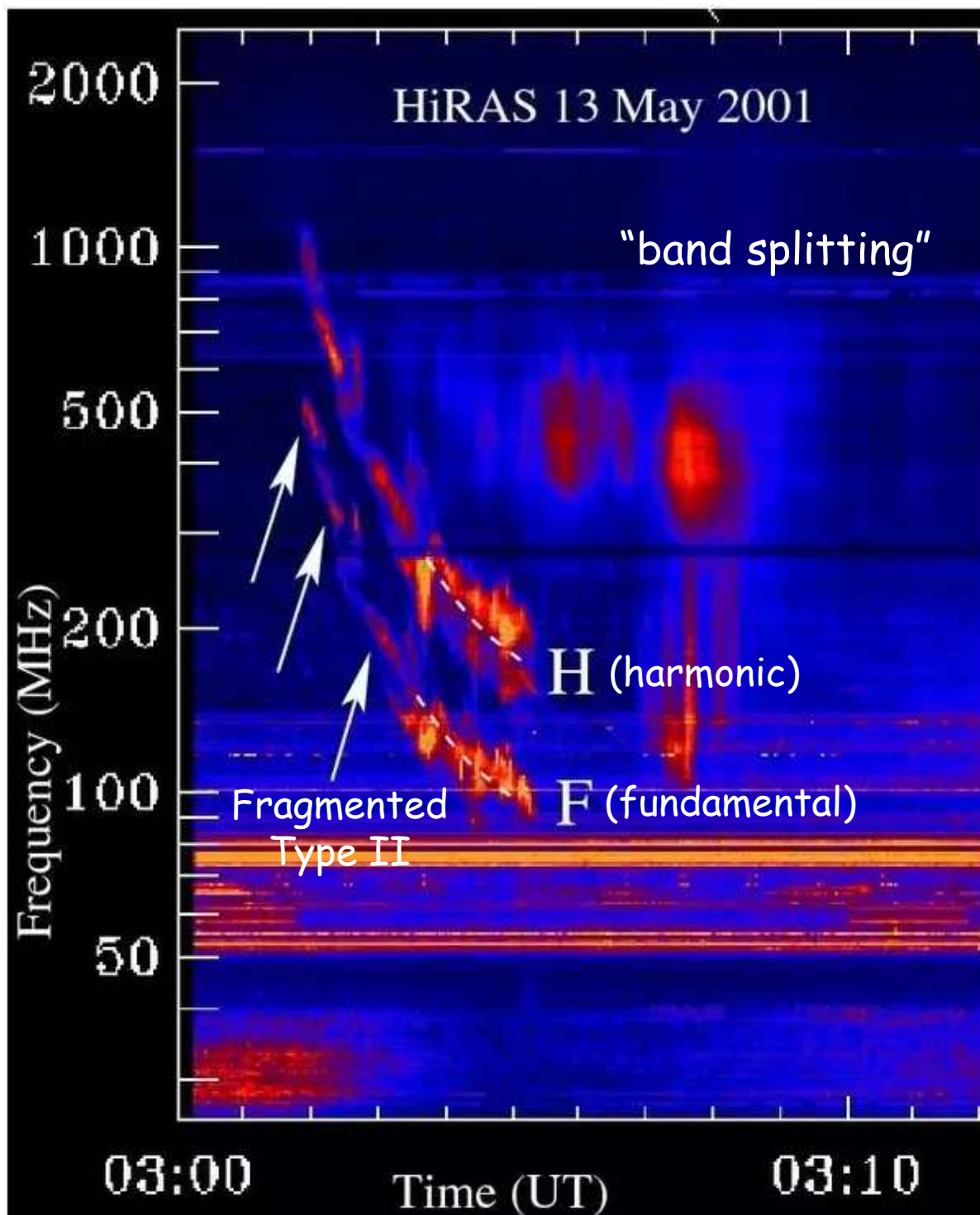


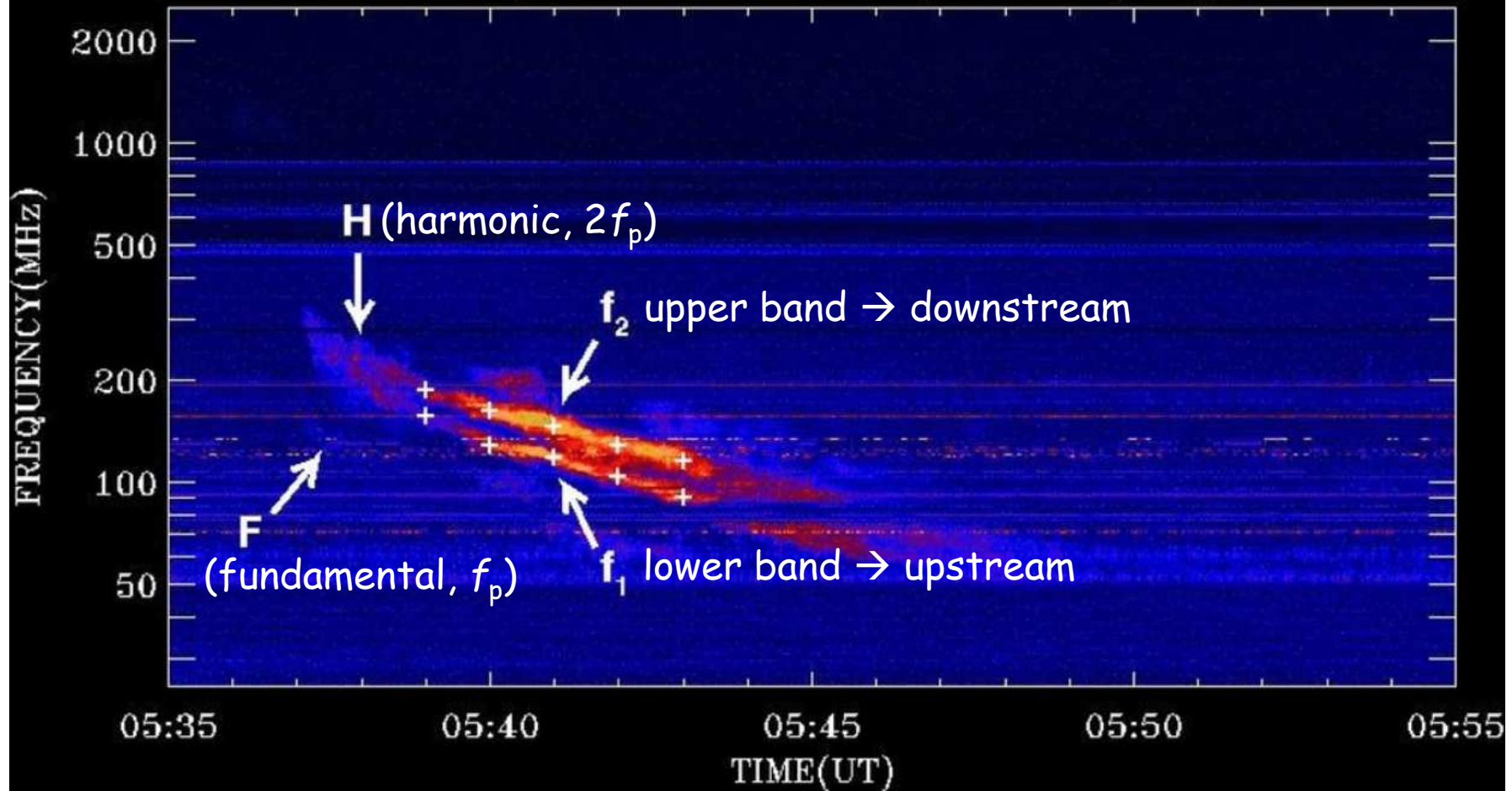
CME Start



Radio-Loud CME





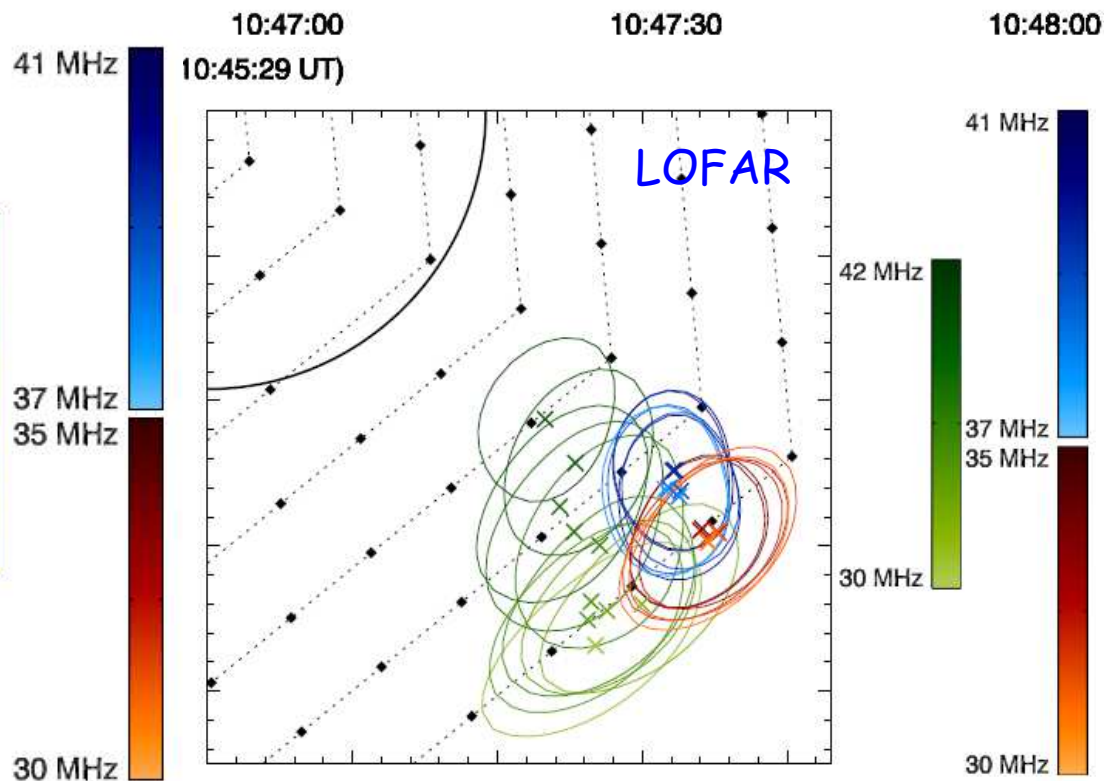
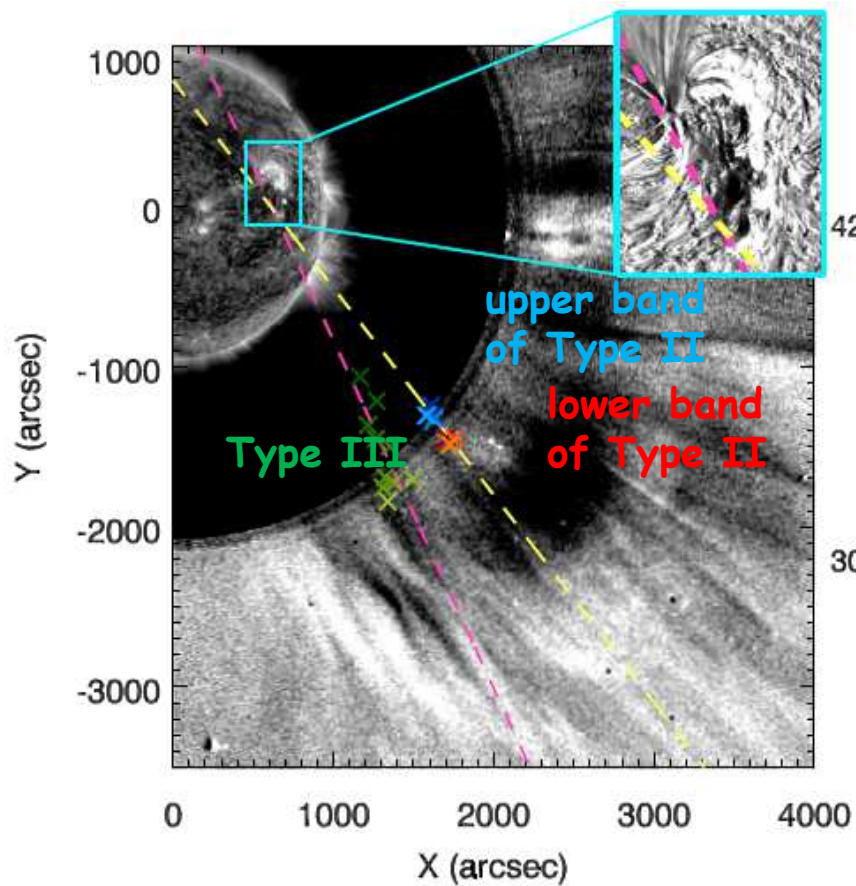
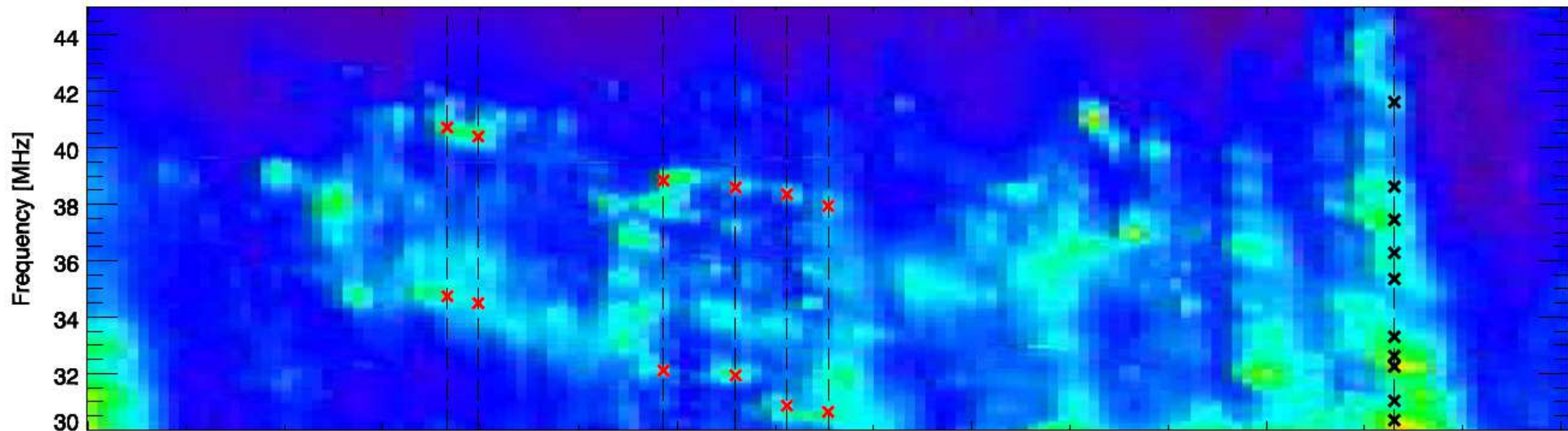


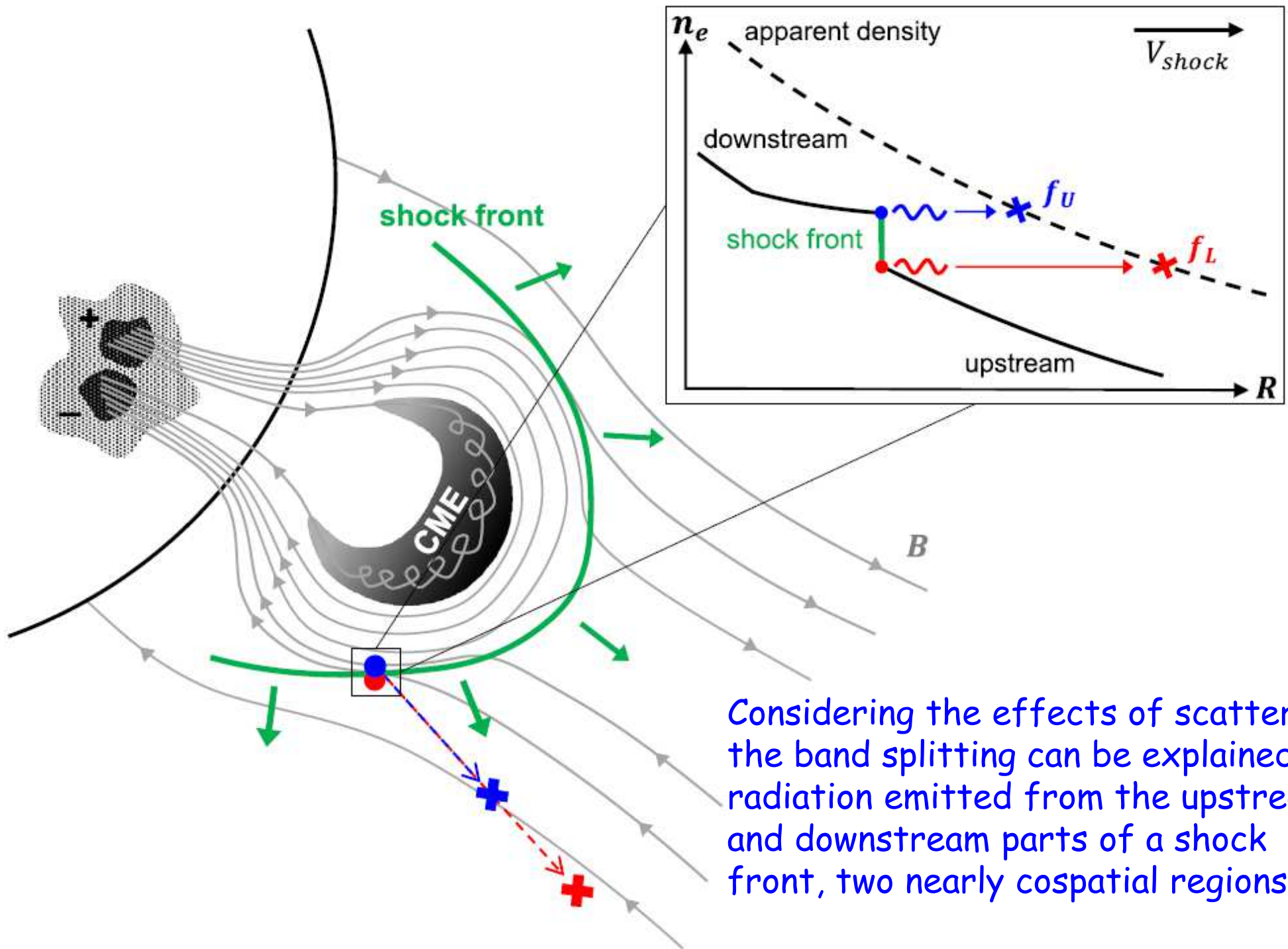
→ $f_p = 9 \times 10^{-3} n^{1/2}$ MHz with the electron density n in cm^{-3}

→ For example, at 05:40 UT, the upper and lower bands of the harmonic component have frequencies $f_2 = 162$ and $f_1 = 128$ MHz, respectively. The local plasma frequencies are therefore $f_{p2} = 81$ and $f_{p1} = 64$ MHz, respectively, corresponds with $n_1 = 5.1 \times 10^7 \text{cm}^{-3}$.

→ shock compression ratio n_2/n_1 is simply $(f_{p2}/f_{p1})^2 = (f_2/f_1)^2$

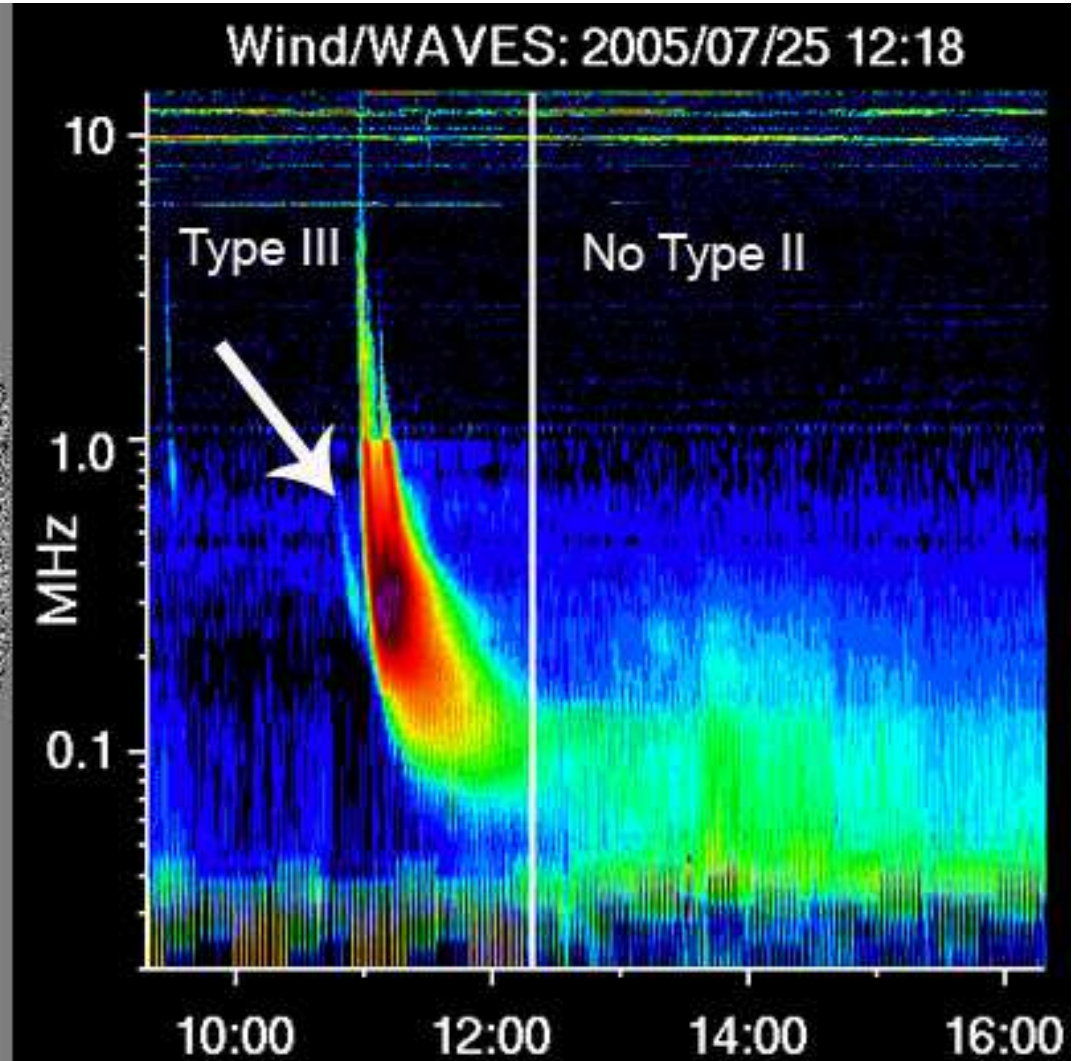
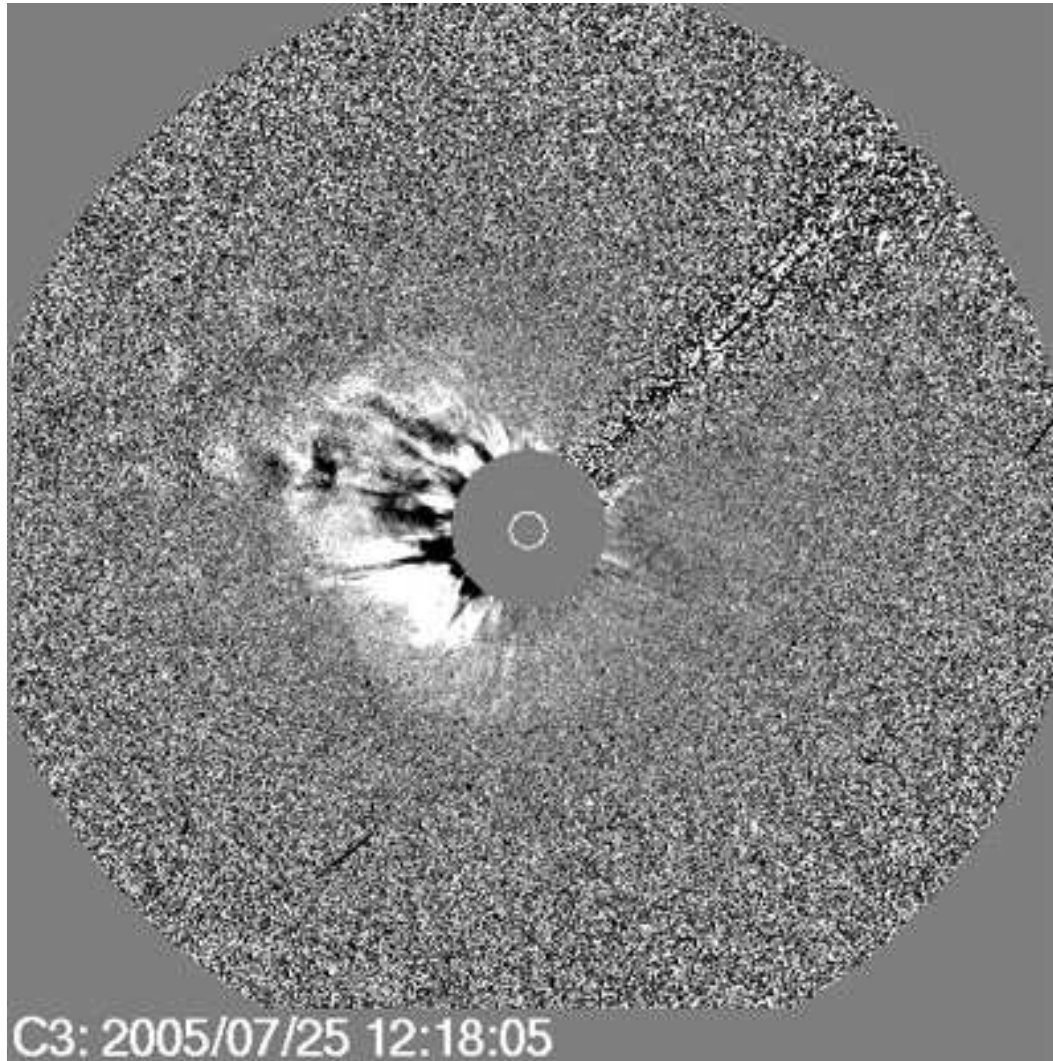
CME on 2015 June 25 near 10:57 UT



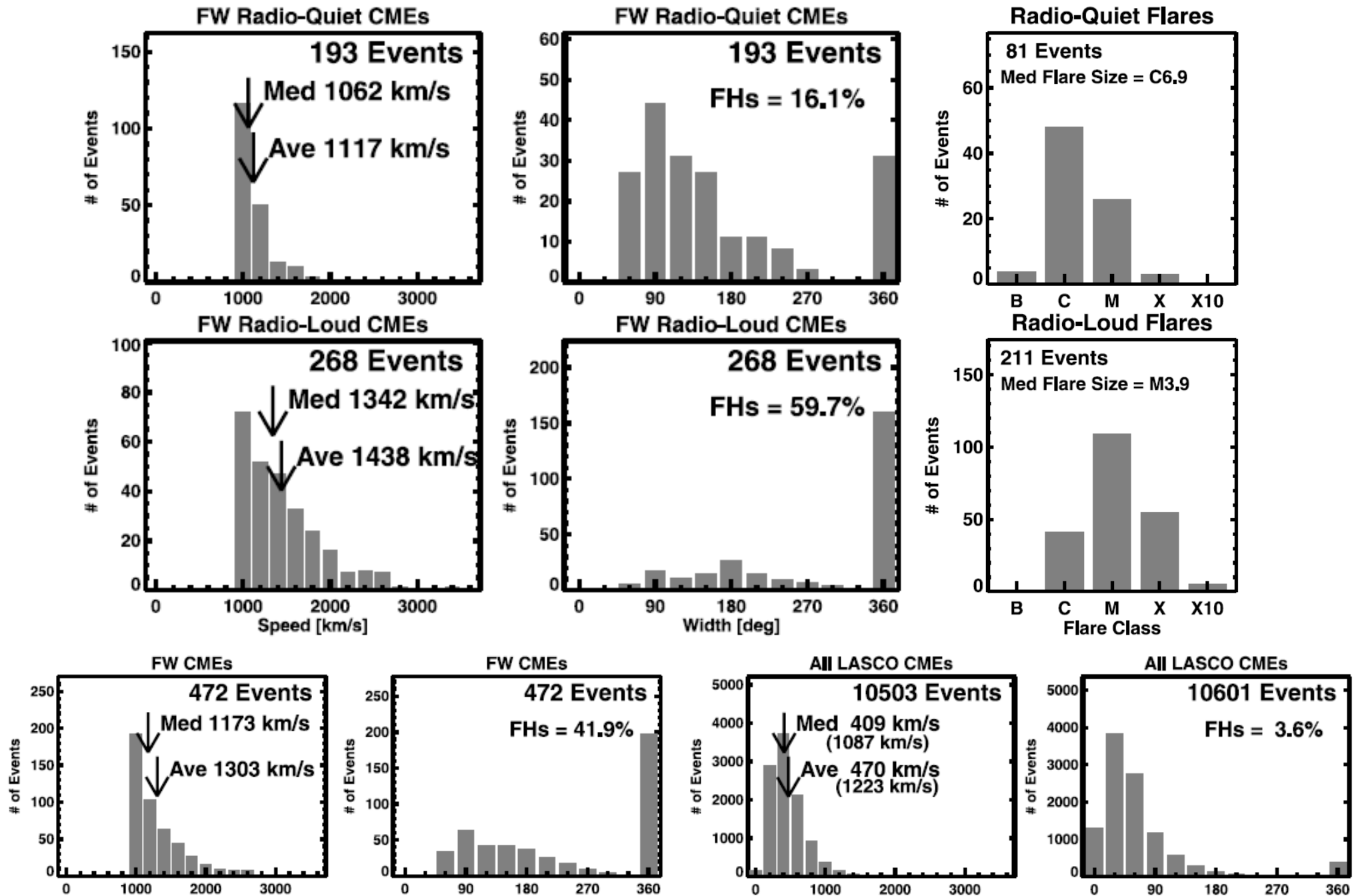


Considering the effects of scattering, the band splitting can be explained as radiation emitted from the upstream and downstream parts of a shock front, two nearly cospatial regions.

Radio-Quiet CME



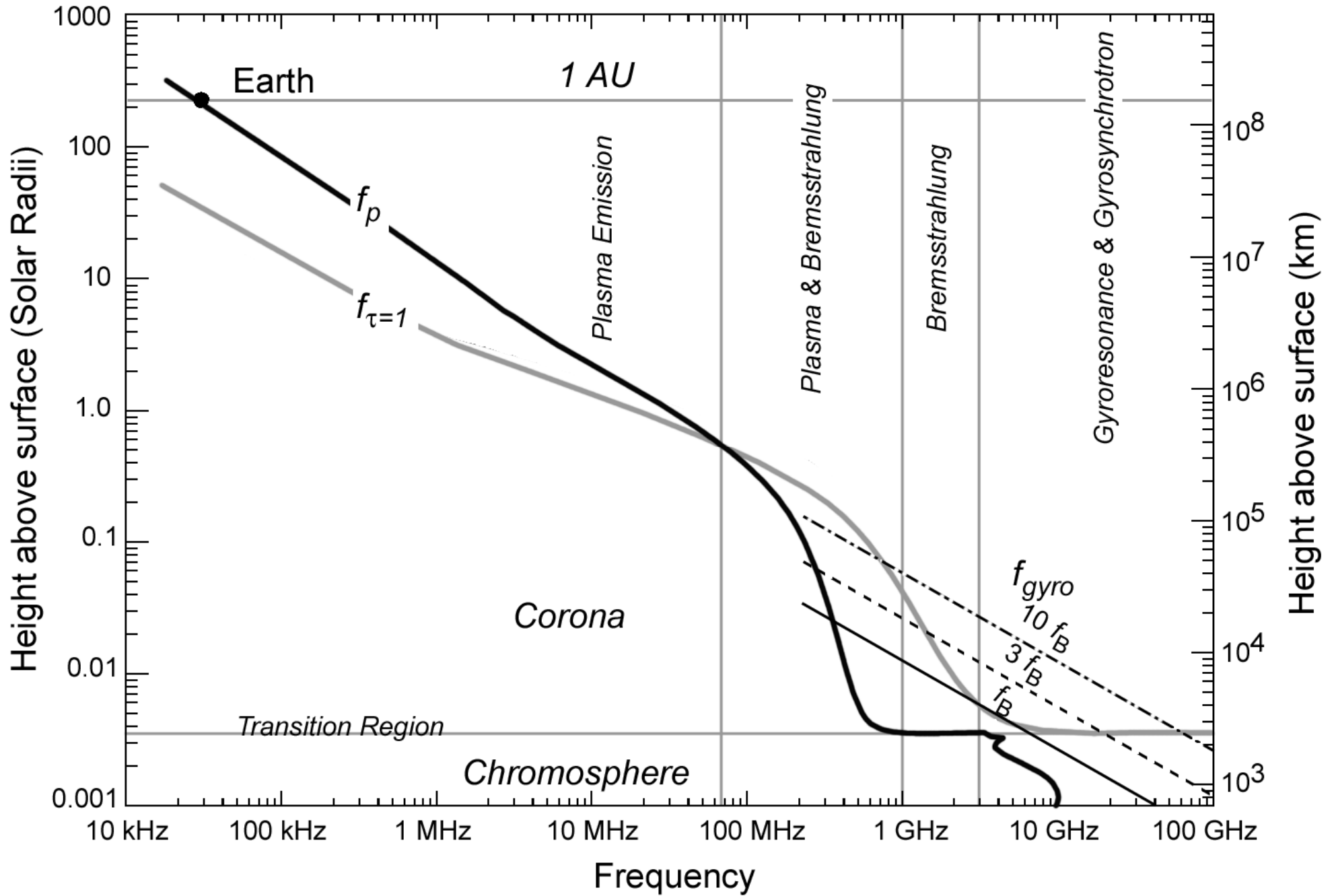
472 fast (speed ≥ 900 km $^{-1}$) and wide (width $\geq 60^\circ$) CMEs during 1996 - 2005 by SOHO/LASCO



552 events from 891 fast CME events (speed \geq 900 km/s) during 1996 - 2012 by SOHO/LASCO

CME properties	Mean values		Flare properties	Mean values	
	Class-D	Class-A		Class-D	Class-A
<i>Radio-quiet</i>			<i>Radio-quiet</i>		
Position angle (degree)	188	175	Duration (min)	33	70
Width (degree)	128.7	128	T_{rise} (min)	16	34
Speed (km s^{-1})	1092	1093	T_{decay} (min)	16	35
Acceleration (m s^{-2})	-25.89	18.59	X	5.79 %	0 %
Initial acceleration (km s^{-2})	1.89	1.56	M	34.78 %	33.33 %
Initial speed (km s^{-1})	1254	951	C	59.42 %	66.66 %
Number of halo events	12.64 %	9.52 %			
<i>Radio-loud</i>			<i>Radio-loud</i>		
Position angle (degree)	209	171	Duration (min)	48	80
Width (degree)	279	310	T_{rise} (min)	25	39
Speed (km s^{-1})	1368	1348	T_{decay} (min)	22	41
Acceleration (m s^{-2})	-32.63	24.96	X	31.7 %	24.48 %
Initial acceleration (km s^{-2})	1.53	0.87	M	48.78 %	46.93 %
Initial speed (km s^{-1})	1567	1094	C	18.2 %	26.53 %
Number of halo events	65.17 %	68.85 %			

RQ CMEs were found to be less energetic than RL CMEs and are less often associated with intense X-ray flares. This confirms the previous results that RQ CMEs do not often exceed the critical Alfvén speed of 1000 km/s in the outer corona that is needed to produce type II radio bursts.



Energetic Particles in the Heliosphere

